

05,08

Detection of spin-wave excitations of a domain structure in an yttrium-iron garnet film using the inverse spin Hall effect

© S.L. Vysotskii^{1,2}, M.E. Seleznev¹, Yu.V. Nikulin^{1,2}, A.V. Kozhevnikov¹,
G.M. Amahanov^{1,3}, A.G. Temiryazev⁴

¹ Saratov Branch, Kotel'nikov Institute of Radio Engineering and Electronics, Russian Academy of Sciences, Saratov, Russia

² Saratov National Research State University, Saratov, Russia

³ Yuri Gagarin State Technical University of Saratov, Saratov, Russia

⁴ Fryazino Branch, Kotel'nikov Institute of Radio Engineering and Electronics, Russian Academy of Sciences, Fryazino, Moscow oblast, Russia

E-mail: vysotsl@gmail.com

Received April 18, 2024

Revised April 18, 2024

Accepted May 8, 2024

Using the inverse spin Hall effect, the generation of EMF in a waveguide cut from an epitaxial film of yttrium-iron garnet (YIG) of crystallographic orientation (111) with a thickness of $15.6\ \mu\text{m}$ and dimensions of $10 \times 5\ \text{mm}$ was studied, on the surface of which a strip of platinum with a thickness of $4\ \text{nm}$, a width of $25\ \mu\text{m}$ and a length of $4\ \text{mm}$ was deposited, when used as a pump spin-wave excitations of the domain structure. The magnetization field tangent to the surface of the structure was directed parallel to the crystallographic axis $(1\bar{1}0)$ of the YIG film. The possibility of EMF registration is shown both in the case of in-phase and antiphase magnetization oscillations in domains and for domain walls' displacement waves. The dependence of the measured EMF level on the type of spin-wave excitation and the magnitude of the magnetization field is investigated. It is shown that the volt-watt sensitivity (the ratio of EMF to the power of spin-wave excitation) can be comparable with a similar parameter for saturated YIG films.

Keywords: magnetostatic surface waves, epitaxial film of yttrium-iron garnet, magnetic domains, platinum.

DOI: 10.61011/PSS.2024.07.58970.34HH

1. Introduction

Generation of charge-carrier current in Platinum film applied on yttrium-iron garnet (YIG) film surface due to the inverse spin Hall effect [1] is of great interest for creation of an energy-efficient element base using spintronics principles [2]. In such a structure, both under resonance microwave pumping [3–5], and excitation of spin waves (SW) in YIG film [6–8] the charge-carrier current is generated in the Platinum film

$$\mathbf{I}_e \propto |I_{s,n}| [\mathbf{n} \times \mathbf{m}], \quad (1)$$

where \mathbf{n} and \mathbf{m} — unit vectors along the normal to YIG film surface and magnetization vectors, $I_{s,n}$ — spin current component along the normal \mathbf{n} . The measured value in this study is $U = I_e R$, where R — resistance of Platinum film. Most often ISHE is studied when magnetization fields values are H which is sufficient for both, magnetization of YIG film to saturation, and prohibition of the three-magnon parametric instability processes [9] which limit the value U [10]. When the field value H decreases to $H < H_s$, where H_s — saturation field, in the YIG film there arise the domain structures capable of supporting the spin-wave excitation due to in-phase and opposite oscillations of

magnetization in domains (DS) as well as due to domain boundaries displacement waves [11–20]. Small values H necessary for their monitoring are interesting in terms of perspective of ISHE use in DS in spintronics devices. Possibility of EMF generation in YIG structures —Pt at $H < H_s$ was described in [21], however, ISHE singularity and dependence of its efficiency for various kinds of spin-wave excitations during bias field tuning was not analyzed.

This paper studies the generation of EMF in YIG structure (111)–Pt based on inverse spin Hall effect when the YIG film is magnetized in direction of easy axis $(1\bar{1}0)$ with the values of bias field H , lower than saturation field.

2. Examined samples and experimental procedure

The structure based on YIG film of crystal-lattice orientation (111) and thickness of $15.6\ \mu\text{m}$ was studied, with magnetization saturation of $4\pi M = 1750\ \text{G}$. A waveguide was cut from the film with flat dimensions $10 \times 5\ \text{mm}$, on the surface of which the magnetron sputtering, photolithography and ion etching processes were used to fabricate a $4\ \text{nm}$ thick, $4\ \text{mm}$ long, $25\ \mu\text{m}$ wide Platinum strip oriented along

the longer side of the waveguide, with its resistance equal $\sim 12\text{ k}\Omega$. The structure was placed into the magnetostatic surface wave (MSSW) delay line mockup (further in the text — mockup) with wire antennas of diameter $40\text{ }\mu\text{m}$ and 7 mm spacing between them which was placed between the electromagnet poles. The bias field was oriented perpendicular to the long axis of the waveguide which corresponded to the equipped with a polarizer direction of crystallographic axis $\langle 1\bar{1}0 \rangle$. A LED matrix was placed under the mockup the light of which dropped on the YIG structure—Pt through the hole in the mockup base. The light that has passed through the structure dropped on the polarization microscope analyzer where digital camera was placed to the eyepiece to register the obtained image. Wire contacts for EMF measurement were attached to the platinum strip by means of conductive glue. Measurements of frequency dependencies of module $S_{12}(f)$ and phase $S_{12}^{\phi}(f)$ of the mockup transfer coefficient were carried out using a vector network analyzer M9374A with power $P_{in} \approx 30\text{ dBm}$ supplied to the antenna. Also frequency dependencies of power $S_{22}(f)$ reflected from the input antenna were registered. EMF frequency dependencies were measured at $P_{in} \approx 7\text{ dBm}$ for increasing the level of registered signal. Microwave power modulation with a 11.3 kHz meander signal allowed measuring of EMF with the help of synchronous detector.

The type of domain structure was studied using a polarization microscope (during measurements of both $S_{12}(f)$ and $U(f)$), at that, using the eyepieces of various magnification degree allowed both, looking at the DS in details, and monitoring of a larger area across the platinum strip to control possible formation of a block structure [12]. The surface morphology of DS was studied using atomic force microscopy (AFM).

During measurements the studied structure was magnetized in field $H = 110\text{ Oe}$, and after that the value H decreased. With selected values H the frequency dependencies of the spin-wave excitations (SWE) and DS image were recorded similar to [12–17]. In our case we have additionally registered the frequency dependence of EMF induced in the Platinum strip.

3. Measurement results

In Figure 1, *a* the curve 1 shows dependence $S_{12}(f)$ of MSSW for $H = 110\text{ Oe}$, when YIG film is in saturated state. The lower edge of MSSW monitoring bandwidth is illustrated in Figure 1, *a* by arrow and designated as $f_1 = 1.23\text{ GHz}$. Let's designate the MSSW monitoring bandwidth in YIG film as SWE1 (spin-wave excitation 1).

When H changes to $H_s \approx 61\text{ Oe}$ (Figure 1, *b*) frequency f_1 goes down to 0.945 GHz . Further decrease of H to $H_1 \approx 60\text{ Oe}$ leads to SWE1 monitoring bandwidth separation in two areas SWE2 and SWE3 with low-frequency boundaries f_2 and f_3 — see curve 1 in Figure 1, *c* for $H = 55\text{ Oe}$. SWE2 monitoring bandwidth is observed when

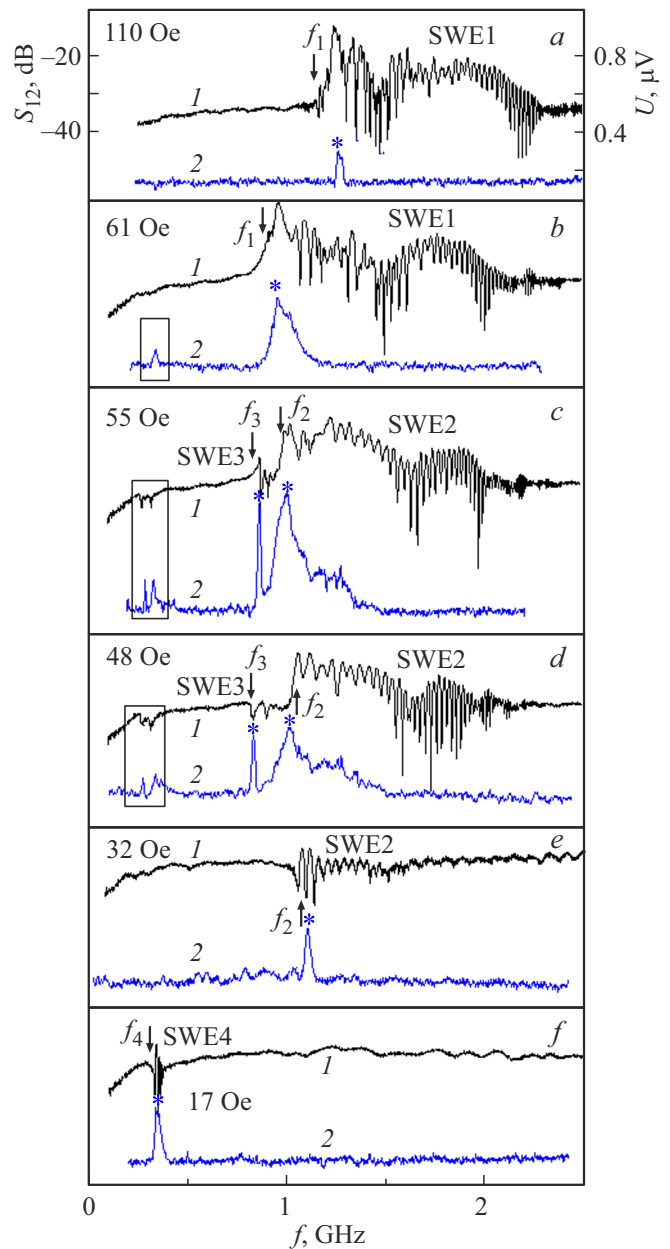


Figure 1. Frequency dependencies of the modulus transfer coefficient $S_{12}(f)$ (curves 1) and EMF (curves 2) for the input power ~ 30 and $\sim 7\text{ dBm}$ respectively, with the values shown in H .

H decreases to $H_2 = 32\text{ Oe}$, while frequency f_2 increases to 1.07 GHz (see curves 1 in Figure 1, *c–e*). SWE3 monitoring bandwidth cannot be recorded when H goes down to $H = 40\text{ Oe}$, while frequency $f_2 = 0.78\text{ GHz}$. In the range $H_3 = 26 < H < H_2 = 32\text{ Oe}$ no any induction signals were observed at the output antenna.

When $3\text{ Oe} < H < H_3$ in $0.3–0.35\text{ GHz}$ band the SWE4 is observed (see Figure 1, *f* for $H = 17\text{ Oe}$). Dependence of frequencies $f_1–f_4$ from H is illustrated in Figure 2, *a*. It is seen that for SWE $f_1–f_3$ they have an almost monotonous nature, while frequency f_4 , equal at 26 Oe to 0.329 GHz

when H decreases to 15 Oe increases to 0.35 GHz, while further it goes down to 0.3 GHz at $H = 3$ Oe.

It should be noted that harmonics in the spectrum of output signal of network analyzer may have impacted the measurements results. Thus the third order harmonic was only by 10 dB lower than the pumping level signal f_{gen} . Thus, when scanning in the bandwidth near $f_{\text{gen}} \approx 0.3$ GHz the third harmonic frequencies ~ 0.9 GHz within $40 < H < 60$ Oe entered into SWE2 and SWE3 band which resulted in registration at frequencies ~ 0.3 GHz of both, the signal $S_{12}(f)$ and $U(f)$ (see highlighted windows in Figure 1, *c* and *d*). Further in this paper these spurious signals are not considered.

It shall be stressed that for SWE1 at $110 \text{ Oe} > H > H_s$ caused by third harmonic the signals are not observed (see Figure 1, *a*), apparently because of limited power of MSW due to three-magnon processes [9]. In case of SWE2 and SWE3 the spurious signals may occur because in the domain structures the threshold power for development of non-linear processes are higher than for the saturated films [12].

It shall be noted that the levels of the second, fourth and further harmonics were at least by 20 dB lower than for f_{gen} . The presence of these harmonics in the experiment didn't influence the measurement results.

In Figure 1, *a–f* the curves 2 illustrate for the given values H the frequency dependencies $U(f)$. It is seen that EMF is induced in all described SWE. Dependencies of maximal value U^* for each kind of SWE (designated by asterisks in figures) from H are given in Figure 2, *b*. It can be seen that for curves 2–4 corresponding to the unsaturated state of YIG film the registered values may exceed the results shown in curve 1 for a saturated film.

Figure 3 shows the image of DS of the studied structure for several values H .

It shall be noted that it is possible to observe the domain structure using Faraday effect due to a difference in signs of normal magnetization component in adjacent domains. However, EMF registration according to ISHE mechanism suggests that there's a magnetization component in the film surface being tangent thereto. In our opinion, this component has the same signs in the domains, since, otherwise averaging of the effect along the strip length shall lead to zero EMF. Also change of the sign of the generated EMF itself during change of direction H also speaks in favor of this theory [21].

It shall be noted that in studies with the help of polarization microscope the domain structures at $H < H_s$ become distinct only when H is reduced to ~ 33 Oe (see Figure 2), the DS period being $\Lambda \approx 10 \mu\text{m}$, an the domain structure itself is a strip structure non-symmetrical with the ratios of „light“ and „dark“ domains ~ 2 (Figure 3, *b*). When $H < 31$ Oe the DS was a symmetrical strip with a period of $\Lambda \approx 10 \mu\text{m}$, which remained the same until $H = 0$ (see Figure 3, *c* and *d*). Dark horizontal strip in Figure 3, *a–d* — is Platinum strip with the width of ($25 \mu\text{m}$) that may be used as a scale mark. (Images are obtained with lenses of

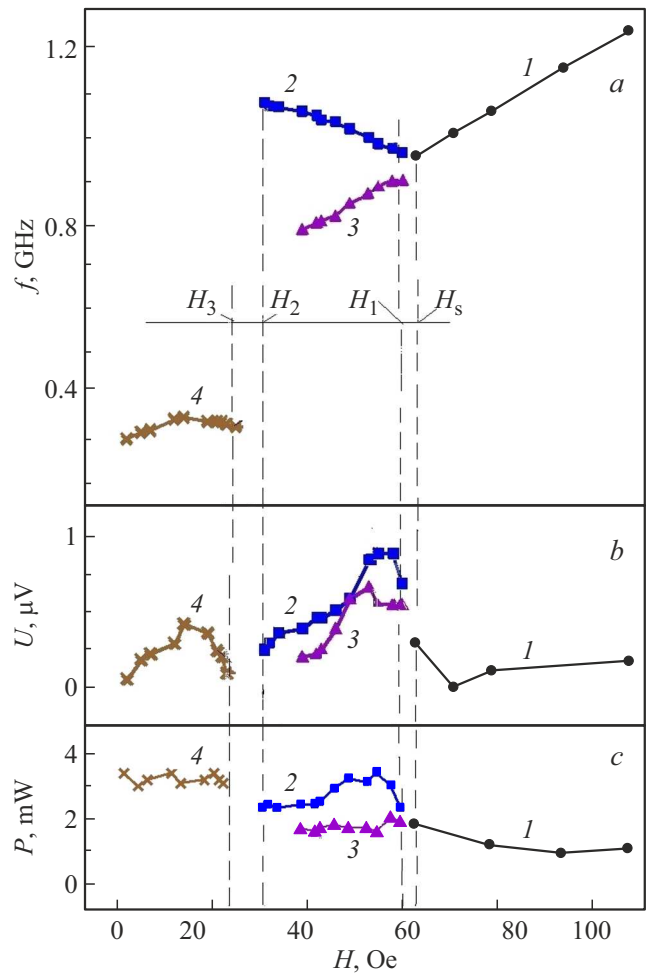


Figure 2. Dependencies from H *a*) frequencies $f_1–f_4$, *b*) EMF, *c*) power consumed for excitation of SWE. The numbers next to the curves correspond to the number of SWE.

various magnification). It shall be noted that presence of Platinum on the surface of YIG film in the studied samples doesn't influence the type of DS.

It shall be emphasized that in the interval $33 \text{ Oe} < H < H_s$ the domain structure could be observed using magnetic force microscopy method (MFM) — see Figure 3, *e* for $H \approx 50$ Oe. Moreover, this method also allows observing the thin surface domain structure (see Figure 3, *f* for $H \approx 10$ Oe). The study of its impacting the SWE characteristics is beyond the scope of this paper.

4. Discussion

First of all, we shall say that both, described changes of domain structure, intervals of magnetic fields proving the existence of specific DS, and the nature of the spin-wave excitation frequencies variation with the change of H are well consistent with the known results [14–16]. At that, we may suggest that SWE2 and SWE3 observed in the experiment occur due to opposite-phase and in-phase

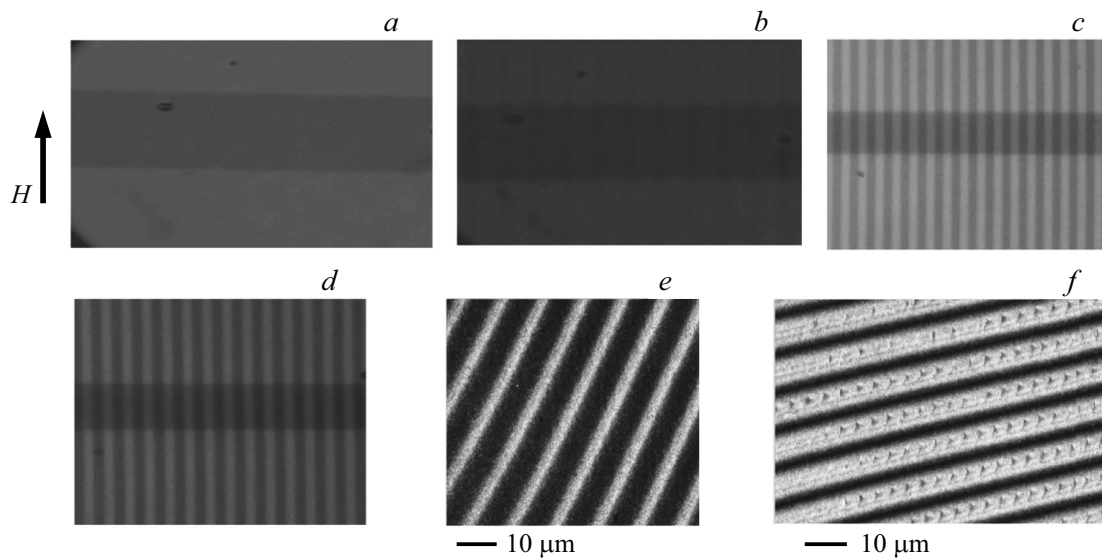


Figure 3. The images of domain structures obtained with the help of a polarization microscope in *a*) 110 Oe, *b*) 33 Oe, *c*) 28 Oe, *d*) 3 Oe using magnetic force microscopy in *e*) 50 Oe and *f*) 10 Oe. The width of the dark horizontal strip in *a*–*d* is equal 25 μm .

magnetization oscillations in the domains, while SWE4 is a domain boundaries bias wave [17–19].

In Figures 1 and 2 we may see that all SWE observed in the studied structure are accompanied with generation of EMF, whereas within H interval of monitoring this or another SWE the plotted curves $U(H)$ have maximum (see Figure 2, *b*). Let's discuss possible reasons of U dependence for SWE2–SWE4 from H .

It is well known that the level of generated EMF is proportional to MSW power P [10]. We have assessed the value P as a difference of power reflected from the input antenna at values H , complying with the experiment conditions and at $H_0 \gg H$ using $S_{22}(f)$ dependence. In Figure 2, *c* we have obtained results shown for SWE1–SWE4. We may see that in H interval of observing SWE2 the power P changes in 1.5 times, while EMF changes in 3.5 times, and for SWE4 the value P changes in 1.1 times, and EMF changes in 7 times. Thus, the described changes of value U are not related to the power versus frequency ratio P . Also it should be noted that for SWE2 the volt-watt sensitivity (EMF to power ratio P) reaches $2 \cdot 10^{-4} \text{ V/W}$, which is equivalent to the similar parameter for saturated YIG films [10]. We suppose that $U(H)$ dependence traces the magnetization direction change \mathbf{m} — in domains when rearranging the DS with change H and, thus, may influence the value \mathbf{I}_e , defined according to (1).

5. Conclusion

EMF generation in Platinum film applied on YIG film surface in saturated state was studied. It is demonstrated that generation is possible for all considered kinds of spin-wave excitations of domain structures. In the studied structure the most efficient generation is observed with the

values of bias field by 5–10 Oe lower than the values of saturation field, as well as in case of formation of a strip-like symmetrical domain structure in YIG film. In the first case the volt-watt sensitivity (EMF to spin-wave excitation power ratio) may be of the same level as equivalent parameter for saturated YIG films [10].

We suppose that the study of domain structures by ISHE method may be useful for diagnostics of domains magnetization state along with other methods of its study.

Funding

This study was supported by grant No. 24-29-00640 from the Russian Science Foundation. The surface domain structures were studied with the use of a probe microscope by A.G. Timiryazev within the state task of Radioelectronics Institute named after V.A. Kotelnikov of the Russian Academy of Sciences.

Conflict of interest

The authors declare that they have no conflict of interest.

References

- [1] M.I. Dyakonov, V.I. Perel. Phys. Lett. A **35**, 6, 459 (1971).
- [2] A. Hirohata, K. Yamada, Y. Nakatani, I.-L. Prejbeanu, B. Diény, P. Pirro, B. Hillebrands. JMMM **509**, 166711 (2020).
- [3] F. Yang, P.C. Hammel. J. Phys. D **51**, 25, 253001 (2018).
- [4] C.W. Sandweg, Y. Kajiwara, K. Ando, E. Saitoh, B. Hillebrands. Appl. Phys. Lett. **97**, 25, 252504 (2010).
- [5] K.Y. Constantinian, G.A. Ovsiannikov, K.L. Stankevich, T.A. Shaikhulov, V.A. Shmakov, A.A. Klimov. Phys. Solid State **63**, 9, 1432 (2021).

- [6] S.A. Manuilov, C.H. Du, R. Adur, H.L. Wang, V.P. Bhallamuid, F.Y. Yang, P.C. Hammel. *Appl. Phys. Lett.* **107**, 4, 042405 (2015).
- [7] A.V. Chumak, A.A. Serga, M.B. Jungfleisch, R. Neb, D.A. Bozhko, V.S. Tiberkevich, B. Hillebrands. *Appl. Phys. Lett.* **100**, 8, 082405 (2012).
- [8] M.B. Jungfleisch, A.V. Chumak, A. Kehlberger, V. Lauer, D.H. Kim, M.C. Onbasli, C.A. Ross, M. Klaui, B. Hillebrands. *Phys. Rev. B* **91**, 13, 134407 (2015).
- [9] A.G. Gurevich, G.A. Melkov. *Magnitnye kolebaniya i volny*, Fizmatlit, M. (1994). 464 p. (in Russian).
- [10] M.E. Seleznev, Y.V. Nikulin, Y.V. Khivintsev, S.L. Vysotsky, A.V. Kozhevnikov, V.K. Sakharov, G.M. Dudko, Y.A. Filimonov. *Izv. vuzov. PND* **31**, 2, 225 (2023). (in Russian).
- [11] Yu.V. Gulyaev, P.E. Zilberman, G.T. Kazakov, V.V. Tikhonov. *Pis'ma v ZhTF* **11**, 1, 97 (1985). (in Russian).
- [12] P.E. Zil'berman, V.M. Kulikov, V.V. Tikhonov, I.V. Shein. *JETP* **72**, 5, 874 (1991).
- [13] A.V. Vashkovskii, É.G. Lokk, V.I. Shcheglov. *Phys. Solid State* **41**, 11, 1868 (1999).
- [14] A.V. Vashkovskii, É.G. Lokk, V.I. Shcheglov. *JETP Lett.* **63**, 7, 572 (1996).
- [15] A.V. Vashkovskii, É.G. Lokk, V.I. Shcheglov. *JETP* **84**, 3, 560 (1997).
- [16] A.V. Vashkovskii, É.G. Lokk, V.I. Shcheglov. *JETP* **87**, 4, 776 (1998).
- [17] S.A. Vyzulin, S.A. Kirov, N.E. Syriev. *Radiotekhnika i elektronika*, **30**, 1 179 (1985). (in Russian).
- [18] D.D. Stancil. *J. Appl. Phys.* **56**, 6, 1775 (1984).
- [19] M. Ramesh, E. Jedryka, P.E. Wigen, M. Shone. *J. Appl. Phys.* **57**, 8, 3701 (1985).
- [20] S.A. Kirov, A.I. Pilschikov, N.E. Syriev. *FTT* **16**, 10, 3051 (1974). (in Russian).
- [21] Y.V. Nikulin, A.V. Kozhevnikov, S.L. Vysotskii, A.G. Temiryazev, M.E. Seleznev, Y.V. Khivintsev, Y.A. Filimonov. *Phys. Solid State* **65**, 7, 1129 (2023).

Translated by T.Zorina